New Observational Constraints for Atmospheric Hydroxyl on Global and Hemispheric Scales

S. A. Montzka,[1]* C. M. Spivakovsky,[2] J. H. Butler,[1] J. W. Elkins,[1] L. T. Lock,[3] D. J. Mondeel[3]

Dramatic declines in emissions of methyl chloroform (1,1,1-trichloroethane) resulting from the Montreal Protocol provide an unprecedented opportunity to improve our understanding of the oxidizing power of Earth's atmosphere. Atmospheric observations of this industrial gas during the late 1990s yield new insights into the global burden and distribution of the hydroxyl radical. Our results set firm upper limits on the global and Southern Hemispheric lifetimes of methyl chloroform and confirm the predominance of hydroxyl in the tropics. Our analysis suggests a global lifetime for methyl chloroform of 5.2 (+0.2, −0.3) years, a Southern Hemispheric lifetime of 4.9 (+0.2, −0.3) years, and mean annual concentrations of OH that are 15 ± 10% higher south of the intertropical convergence zone than those north of this natural mixing boundary between the hemispheres.

The hydroxyl radical plays a central role in the chemistry of Earth's atmosphere (*1*). This powerful oxidant initiates photochemical reactions that cleanse the atmosphere of many gases affecting stratospheric ozone and global climate, and it is intimately involved in the production of tropospheric ozone. We show here how atmospheric measurements of CH_3CCl_3 during periods of rapidly declining and small emissions provide a unique opportunity to place constraints on estimates of hydroxyl radical concentrations on global and hemispheric scales.

To that end, we have measured CH_3CCl_3 in air from flask samples collected routinely since 1992 at 7 to 10 remote locations across the globe (Fig. 1) (*2*). In contrast to observations from previous years (*3*–*6*), our recent data reveal only small differences between mean mixing ratios of CH_3CCl_3 in the Northern and Southern Hemispheres and consistently lower mixing ratios in the tropics of both hemispheres than at higher latitudes (*7*) (Figs. 2 and 3). Also, intrahemispheric gradients were similar within both hemispheres during 1998–1999 (Fig. 3), which suggests that the distribution of methyl chloroform is now controlled primarily by atmospheric removal rather than by anthropogenic releases. These recent observations support theoretical predictions of the change in gradient expected with large reductions in emissions (*8*) and confirm the predominance of OH in the tropics. Furthermore, the data provide clear evidence that long-lived reduced gases such as CH_4 and hydrochlorofluorocarbons are destroyed primarily in the tropics.

To date, constraints on the global concentration of OH stem from trend and budget analyses of trace gases that are oxidized primarily by OH, such as CH_3CCl_3, ^{14}CO, and $CHClF_2$ (*3*, *4*, *8*–*12*). The mean global burden of OH calculated in this way, however, depends strongly on the accuracy of calibration and source strength estimates for these gases (*2*–*4*). Because emissions of CH_3CCl_3 have declined rapidly and are now small, we can obtain an estimate of its atmospheric removal rate that is less sensitive to uncertainties in these quantities (*13*). If we consider the globe as a single box, the mean, global, first-order rate constant for removal of a gas from the atmosphere can be expressed as

$$k_g = \frac{E_g}{G} - \frac{(dG/dt)}{G} \qquad (1)$$

where G is the number of moles of a trace gas in the global atmosphere, E_g is the number of moles emitted to the global atmosphere per year, and t is time. After emissions decrease rapidly or cease [that is, when E_g/G is small compared to $(dG/dt)/G$], the relative rate of change approaches k_g as a limit. The inverse of k_g is the mean atmospheric lifetime of the gas. For methyl chloroform, k_g is determined predominantly by OH oxidation in the troposphere but also includes slower losses in the stratosphere (*14*) and in warm waters of the ocean (*15*, *16*).

Our measurements show that the exponential rate of decline for CH_3CCl_3 in the global troposphere was 0.182 year^{-1} during 1998 and 1999, which corresponds to an *e*-fold decay time and a firm upper limit to the global CH_3CCl_3 lifetime of 5.5 ± 0.1 years (1 SD) (*17*) (Fig. 4). Global industrial production and consumption data suggest that E_g/G was only 6% of the observed rate of decay over this period (*18*). In contrast, E_g/G was comparable to or even larger than the atmospheric rate of change during the 1980s and early 1990s (*19*, *20*). On the basis of the observed decay and these emissions, we calculate a global lifetime for CH_3CCl_3 of 5.2 (+0.2, −0.3) years over 1998–1999 (*21*). Because E_g/G was small relative to the observed atmospheric decay over this period [$(dG/dt)/G$], this global lifetime estimate is much less sensitive to calibration accuracy and uncertainties in industrial emissions than are previous lifetime estimates.

The global tropospheric concentration of OH implied by this lifetime estimate is 1.1 (±0.2) × 10^6 rad cm^{-3} (*22*), or slightly lower than can be derived from trend and budget analyses of CH_3CCl_3 and $CHClF_2$ in the presence of substantial emissions (*4*, *8*, *12*). Our results would be consistent with CH_3CCl_3 lifetimes of 4.8 years (*4*) or less (*8*, *12*) and with higher OH concentrations only if emissions of CH_3CCl_3 have been underestimated by about a factor of 3 or more in recent years (*23*). A small portion of this discrepancy could stem from changes in the global lifetime of CH_3CCl_3 as emissions have declined, either as a result of interannual changes in mean annual OH or because the distribution of this gas in the atmosphere has changed relative to the distribution of sinks in recent years. Such lifetime changes, however, are expected to be small (*2*).

Knowledge of OH concentrations on

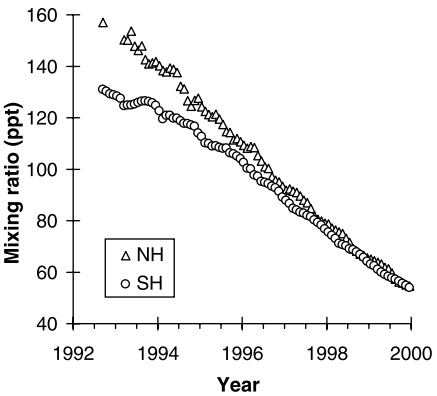

Fig. 1. The measured atmospheric burden of CH_3CCl_3 in recent years. Monthly hemispheric mixing ratios for the Northern (NH, triangles) and Southern (SH, circles) Hemispheres at Earth's surface were calculated as weighted averages of observations from three to six sampling stations in each hemisphere. Since 1997, an average of two pairs per month was collected at each of the sampling sites. For more information, see the supplementary material (*2*). All mixing ratios are reported as parts per trillion by mole (pmol mol^{-1} or ppt).

[1]National Oceanic and Atmospheric Administration, Climate Monitoring and Diagnostics Laboratory, 325 Broadway, Boulder, CO 80303, USA. [2]Department of Earth and Planetary Sciences and Division of Engineering and Applied Sciences, Harvard University, Cambridge, MA 02138, USA. [3]Cooperative Institute for Research in Environmental Sciences, University of Colorado, Boulder, CO 80303, USA.

*To whom correspondence should be addressed.

hemispheric scales is critical for an improved understanding of reduced gases having poorly defined sources—gases such as CH_4, CH_3Br, and CH_3Cl. In the past, our understanding of OH on these spatial scales has contained substantial uncertainty. Estimates of the relative hemispheric concentration of OH based on past observations of CH_3CCl_3 suffered from uncertainties in air exchange rates between the hemispheres and from difficulties in estimating hemispheric burdens of CH_3CCl_3 in the presence of substantial emissions (*8*). Significant uncertainties also remain for inferring the global and relative hemispheric abundance of OH from measurements of ^{14}CO (*8*, *24*). Uncertainties in distributions of precursors and sinks for OH preclude a definitive calculation of the hemispheric partitioning of this oxidant; different models can calculate more OH in either hemisphere (*25*–*28*) or similar amounts in both (*8*, *29*).

Because the net flux of methyl chloroform across the intertropical convergence zone (ITCZ) is now reduced and because Southern Hemispheric emissions continue to account for only a small fraction of global emissions (*18*, *20*), our recent data allow us to place tight constraints on the loss frequency of CH_3CCl_3 in the Southern Hemisphere for the first time. If we consider a two-box model in which the boxes represent the Northern and Southern Hemispheres and are separated at the ITCZ (a natural mixing boundary), mass balance considerations allow us to express the first-order rate constant for loss of methyl chloroform in the Southern Hemisphere as

$$k_s = \frac{E_s}{S} - \frac{(dS/dt)}{S} + k_{ex}\left(\frac{N}{S} - 1\right) \quad (2)$$

where E_s represents Southern Hemispheric emissions, S and N are mean hemispheric mixing ratios (*2*), and k_{ex} is a rate constant for air exchange between the hemispheres. With this approach, the mean decay observed south of the ITCZ and the measured hemispheric difference allow us to estimate a Southern Hemispheric lifetime ($1/k_s$) for CH_3CCl_3 of 4.9 ($+0.2$, -0.3) years during 1998–1999 (*2*, *21*). Emissions south of the ITCZ influence this estimate for $1/k_s$ insignificantly because they accounted for

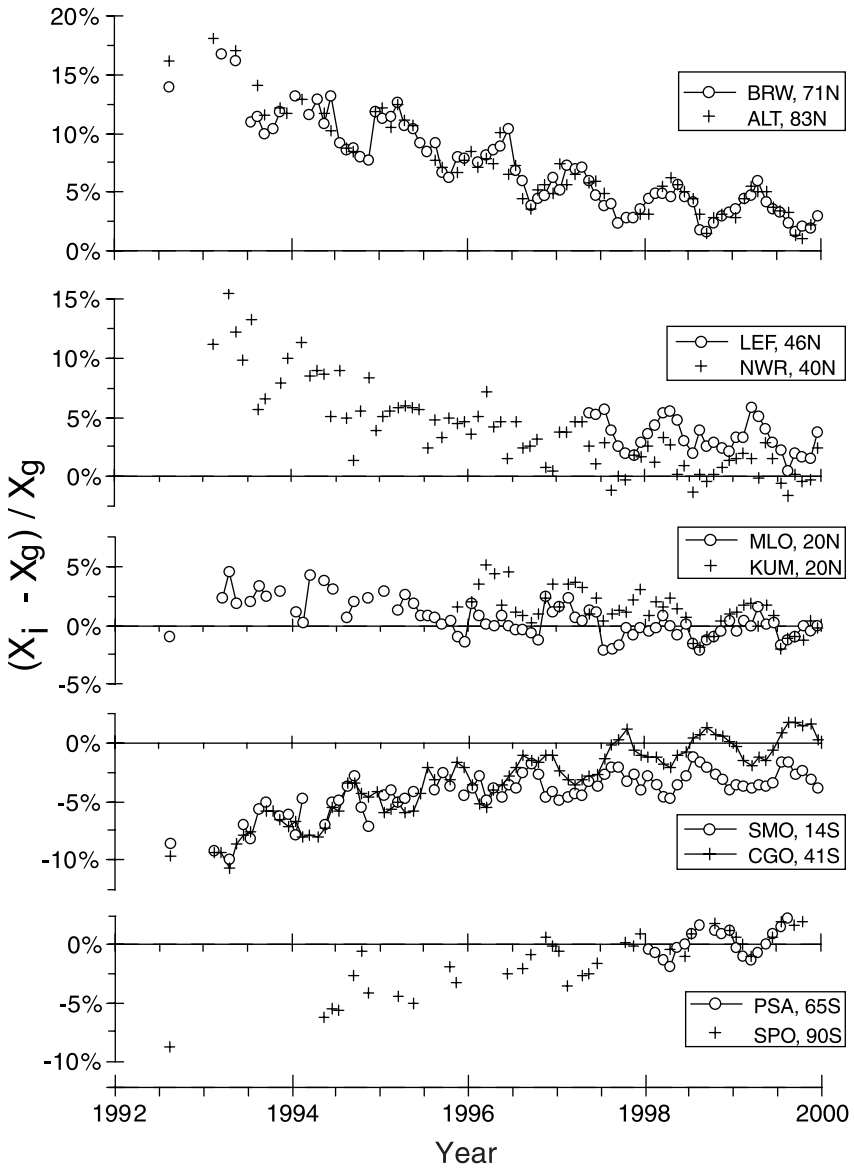

Fig. 2. The changing atmospheric distribution of CH_3CCl_3 at Earth's surface. Relative differences between monthly mean mixing ratios at individual sites (X_i) and global monthly means (X_g) are shown over the period of measurements. Global means were estimated as a simple average of the hemispheric means. Sampling sites and latitudes are indicated in the insets at right. See (*2*) for further details regarding these sampling sites and methods for estimating hemispheric means from these data.

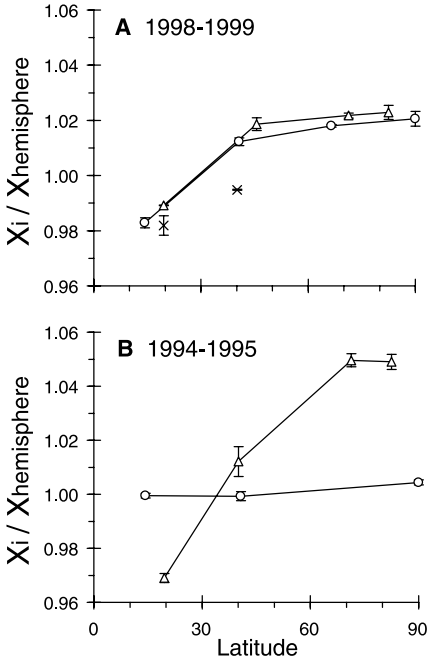

Fig. 3. Measured intrahemispheric gradients in annual mean mixing ratios of CH_3CCl_3. (**A**) Annual means for individual sites (X_i) are shown normalized to respective hemispheric annual means for the years 1998 and 1999. In the Northern Hemisphere (triangles), only data from low-altitude sites (<1000 m) are shown with similar symbols and are connected with lines to allow for appropriate comparisons to similar sites in the Southern Hemisphere (circles). Lower mixing ratios are observed at higher altitude sites (crosses) in the Northern Hemisphere, and this may reflect the presence of continued emissions. Model calculations [(*8*) not shown in the figure], however, predict that similar vertical gradients are expected at midlatitudes even in the absence of emissions, owing to downward transport of CH_3CCl_3-depleted air from the tropics. (**B**) Same as (A) but for the years 1994 and 1995, when Northern Hemispheric emissions were substantial (*19*). Because of a lack of measurements from all sites in this earlier period, data from both low- and high-altitude locations are shown with similar symbols in this panel. Error bars in both panels represent 1 SD of the annual mean ratios estimated for the two years.

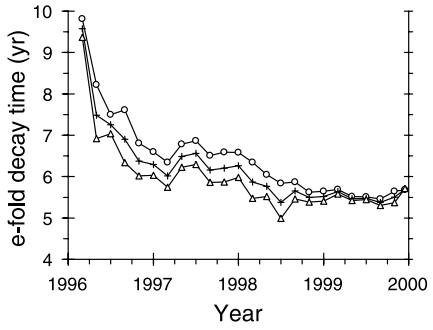

Fig. 4. Global and hemispheric rates of decay expressed as *e*-fold times (*17*). *e*-fold times appear at the end of each yearly period for which *e*-fold times were computed [for example, $\tau_{e,\ 1999.2} = (\ln X_{1999.2} - \ln X_{1998.2})^{-1}$; global *e*-fold times appear as plus signs, Southern Hemisphere times as circles, and Northern Hemisphere times as triangles]. The mean global decay time constant since the beginning of 1998 is estimated at 5.5 ± 0.1 years (*17*).

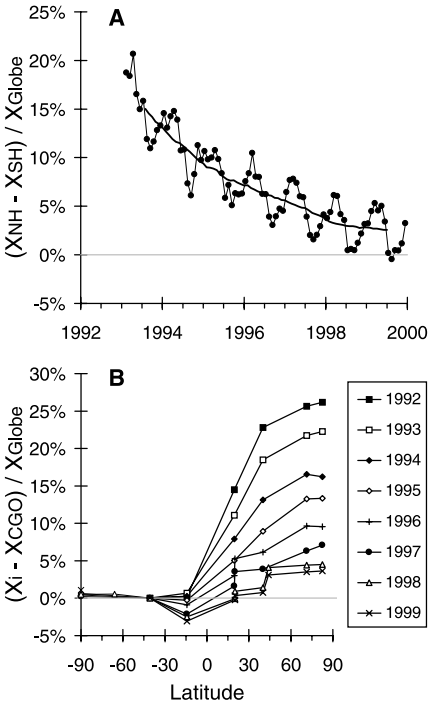

Fig. 5. Measured inter- and intrahemispheric gradients for atmospheric CH_3CCl_3. (**A**) The measured difference between the Northern (X_{NH}) and Southern (X_{SH}) Hemisphere mixing ratios relative to the global mean (X_{Globe}) on a monthly basis. Monthly differences (solid circles) are connected with a thin line; the heavy line represents a 12-month running mean. Our measurements show that the mean annual difference between the two hemispheres was 2.9 ± 0.4% during 1998–1999 (*2*). (**B**) The relative difference in annual mean mixing ratio between each sampling site and Cape Grim (CGO, 41°S), normalized by the annual global mean (X_{Globe}).

Fig. 6. The ratio of hemispheric loss frequencies (k_n/k_s) for CH_3CCl_3 implied by recent measurements. From the global and Southern Hemispheric lifetimes derived in the text, we estimate $k_n/k_s = 0.88 \pm 0.09$ (open circle) (*2*). This estimate is based on atmospheric measurements and industrial emissions over 1998–1999 and on rates of air exchange between the hemispheres [see text and (*2*, *18*)]. Because sinks other than OH oxidation are relatively small and symmetric, k_n/k_s is a good approximation for $\langle OH\rangle_n/\langle OH\rangle_s$ (*2*). Also shown are relative hemispheric loss frequencies implied by the measured hemispheric difference for a range of assumed global emissions and global lifetimes [solid line; see also (*2*)]. Mean concentrations of OH that are 10 to 30% higher in the Northern Hemisphere (*25*, *26*) could be reconciled with our data only if industrial emissions were underestimated by more than a factor of 3 in 1998–1999 and if the global lifetime of CH_3CCl_3 were less than 4.8 years.

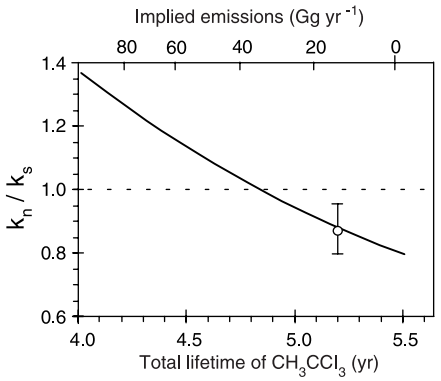

only a small fraction of diminished global emissions over this period (*2*, *18*); E_s/S is estimated to have been only 1% of the observed relative rate of decay [$(dS/dt)/S$] in 1998 and 1999. Northern Hemispheric emissions need not be known in this approach. The accuracy of this hemispheric lifetime estimate does depend on our ability to constrain net hemispheric exchange of CH_3CCl_3 from the measured hemispheric difference and the interhemispheric exchange time $1/k_{ex}$. However, in the absence of the large concentration gradients and variability that arose in the past from substantial emissions, hemispheric means and differences can now be estimated with greater certainty. Furthermore, because the burden of CH_3CCl_3 is similar in the two hemispheres (Fig. 5), uncertainties in k_{ex} now have a small influence on the value calculated for k_s [we estimate that $k_{ex}(N/S - 1)$ was 15 ± 5% of the measured decay during 1998–1999].

The global and hemispheric lifetimes derived from this analysis suggest that the loss frequency of CH_3CCl_3 south of the ITCZ is 15 ± 10% higher than the loss frequency north of this natural boundary between the hemispheres ($k_n/k_s = 0.88 \pm 0.09$). A similar asymmetry in the hemispheric loss frequency of CH_3CCl_3 can also be derived from the hemispheric difference we have measured for this gas during 1998–1999 (Figs. 5 and 6) (*2*). In the presence of significant emissions, hemispheric differences for longer-lived gases are determined predominantly by the magnitude and distribution of these emissions and by air exchange rates between the hemispheres. As emissions become small, however, this difference becomes sensitive to any asymmetry in loss frequencies as well (*2*, *8*). Because losses of methyl chloroform to the ocean and stratosphere are relatively small and symmetric between the hemispheres (*14*–*16*), any significant asymmetry in its loss frequency reflects an asymmetry in the mean hemispheric concentrations of the hydroxyl radical.

Our results suggest that mean annual concentrations of OH south of the ITCZ are 15 ± 10 % higher than they are north of this natural mixing boundary (Fig. 6) (*2*). Because the ITCZ is positioned slightly north of the equator on average, the hemispheric asymmetry in OH would be somewhat smaller if estimated for hemispheres divided at the equator (*30*). Despite this, our findings are not consistent with the significantly higher concentrations in the Northern Hemisphere that are calculated in some models (*25*, *26*) or implied from an analysis of CH_2Cl_2 measurements (*8*), and they suggest that higher concentrations of nitrogen oxides, ozone, and other OH precursors in the Northern Hemisphere are more than balanced by higher loss rates for this important oxidant as well.

References and Notes

1. H. Levy II, *Science* **173**, 141 (1971).
2. For further details, see the supplementary material at *Science* Online at www.sciencemag.org/feature/data/1047766.shl. Our data are available on request or can be found at ftp://ftp.cmdl.noaa.gov/hats/ or through www.cmdl.noaa.gov.
3. R. Prinn *et al.*, *J. Geophys. Res.* **97**, 2445 (1992).
4. R. G. Prinn *et al.*, *Science* **269**, 187 (1995).
5. S. A. Montzka *et al.*, *Science* **272**, 1318 (1996).
6. S. A. Montzka *et al.*, *Nature* **398**, 690 (1999).
7. In the 1980s and early 1990s, mean annual mixing ratios at American Samoa (SMO, 14°S) were generally higher than those at Tasmania (CGO, 41°S) and the South Pole (SPO, 90°S) by an average of 2 to 4% (*3*–*5*). During El Niño years, however, the net flux of CH_3CCl_3 from the Northern to the Southern Hemisphere was reduced at Earth's surface, and similar mixing ratios and seasonality were observed at SMO and CGO (*3*, *4*). We have observed consistently less methyl chloroform at SMO than at CGO since late 1996 in years characterized by El Niño and La Niña conditions (Figs. 2 and 3).
8. C. M. Spivakovsky *et al.*, *J. Geophys. Res.* **105**, 8931 (2000).
9. B. Weinstock and H. Niki, *Science* **176**, 290 (1972).
10. H. B. Singh, *Geophys. Res. Lett.* **4**, 453 (1977).
11. J. E. Lovelock, *Nature* **267**, 32 (1977).
12. B. R. Miller, J. Huang, R. F. Weiss, R. G. Prinn, P. J. Fraser, *J. Geophys. Res.* **103**, 13237 (1998).
13. A. R. Ravishankara and D. L. Albritton, *Science* **269**, 183 (1995).
14. *Scientific Assessment of Ozone Depletion: 1998* (Report No. 44, World Meteorological Organization, Geneva, Switzerland, 1999), chaps. 1 and 2.
15. J. H. Butler *et al.*, *J. Geophys. Res.* **96**, 22347 (1991).
16. S. A. Yvon-Lewis and J. H. Butler, *Eos* **78,** F93 (1997).
17. Reciprocal exponential rates (*e*-fold times in years) were estimated from bimonthly measurements between 1998.0 and 2000.0 and were similar at all sites: SPO, 5.8 ± 0.3; PSA, 5.6 ± 0.1; CGO, 5.6 ± 0.1; SMO, 5.5 ± 0.2; MLO, 5.6 ± 0.1; KUM, 5.5 ± 0.1; NWR, 5.5 ± 0.4; LEF, 5.4 ± 0.3; BRW, 5.4 ± 0.2; ALT,

5.4 ± 0.2; Northern Hemisphere, 5.5 ± 0.1; Southern Hemisphere, 5.6 ± 0.1; globe, 5.5 ± 0.1. The *e*-fold times for SPO and PSA are based on fewer data than for the other sites (*2*). The uncertainties quoted on the global *e*-fold time (1 SD) include a statistical uncertainty in determining the decay exponent and the potential influence of drift in calibration reference standards and detector nonlinearity. See (*2*) for additional discussion of this and other uncertainties. Provided that the OH-CH_3CCl_3 reaction rate constant and the loss rates of methyl chloroform to the ocean and stratosphere are known (*14*–*16*), the observed global *e*-fold time defines a lower limit of 1.0 (±0.2) × 10^6 rad cm^{-3} to mean OH in the global troposphere (*22*) and upper limits to the global lifetimes of other important reduced gases such as CH_4, hydrochlorofluorocarbons (HCFCs), and hydrofluorocarbons (HFCs) that are entirely independent of calibration accuracy and emission figures for CH_3CCl_3 (*2*).

18. Consumption (that is, sales leading to emissions) of CH_3CCl_3 in the Northern Hemisphere during 1995–1998 accounted for 90 to 95% of global consumption (*20*). Here we assume that this ratio is relevant for the distribution of emissions as well. Data contained in these reports (*19*, *20*) have been combined to provide global estimates of emissions through 1998 and projections for likely emissions in 1999 (A. McCulloch, personal communication, 1999). Global emissions of 30 (<40) Gg in 1997, 16 (<24) Gg in 1998, and 13 (<20) Gg in 1999 are calculated from this analysis (numbers in parentheses represent upper limits determined by A. McCulloch after considering accelerated release and higher total production in recent years).
19. P. M. Midgley and A. McCulloch, *Atmos. Environ.* **29**, 1601 (1995).
20. *Production and Consumption of Ozone-Depleting Substances 1986–1998* (United Nations Environment Programme, Nairobi, Kenya, 1999), table 5 (available at www.unep.org/ozone/DataReport99.htm).
21. The stated uncertainty (1 SD) in the estimated global and Southern Hemispheric lifetimes includes global emissions of 15 (+17, −8) Gg $year^{-1}$ in 1998–1999, ±30% in absolute measurement calibration, and the uncertainties discussed in (*2*) and (*17*). The Southern Hemispheric lifetime estimate also includes an additional uncertainty associated with the time it takes for air to exchange between the hemispheres ($1/k_{ex}$ = 1.1 ± 0.3 years) and in the mean hemispheric difference during 1998–1999 of 2.9 ± 0.4% (*2*). The upper limit for emissions used here is larger than suggested in (*18*) to account for the possibility that small amounts of CH_3CCl_3 may be emitted from biomass burning (*31*). Initial upper limits to this emission (*31*) have since been revised downward and suggest that emissions from burning are probably <10 Gg $year^{-1}$ (*32*). Even smaller emissions (<1 Gg $year^{-1}$) can be inferred from emission ratios for CH_3CCl_3 relative to CH_3Cl from burning of grasslands and woods in northern Australia (*33*).
22. Global tropospheric OH concentrations are calculated here from global lifetime estimates for CH_3CCl_3; the rate constant between OH and CH_3CCl_3, evaluated at 270 K (*8*); a partial lifetime for CH_3CCl_3 with respect to oceanic loss of 94 years (*15*, *16*) and with respect to stratospheric loss of 45 years (*14*); and by presuming that the fraction of atmospheric mass in the troposphere is 0.82 ± 0.02. Uncertainties on OH mixing ratios given in the text and in (*17*) include uncertainties in the measured decay rate and in the rate constant between OH and CH_3CCl_3.
23. Emissions inferred from our atmospheric measurements and a lifetime of ≤4.8 years are ≥80 to 90 Gg in 1997, ≥42 to 46 Gg in 1998, and ≥35 to 38 Gg in 1999, or nearly three times more than emissions derived from industrial data (*18*).
24. P. Jöckel, M. G. Lawrence, C. A. M. Brenninkmeijer, *J. Geophys. Res.* **104**, 11733 (1999).
25. S. Houweling, F. Dentener, J. Lelieveld, *J. Geophys. Res.* **103**, 10673 (1998).
26. Y. Wang, J. A. Logan, D. J. Jacob, *J. Geophys. Res.* **103**, 10757 (1998).
27. X. Tie *et al.*, *J. Geophys. Res.* **97**, 20751 (1992).
28. M. L. Gupta, R. J. Cicerone, D. R. Blake, F. S. Rowland, I. S. A. Isaksen, *J. Geophys. Res.* **103**, 28219 (1998).
29. C. M. Spivakovsky *et al.*, *J. Geophys. Res.* **95**, 18441 (1990).
30. The ratio $\langle OH\rangle_n/\langle OH\rangle_s$ inferred from trace gas measurements is relevant for hemispheres divided at the natural mixing boundary, the ITCZ. In models, asymmetry in hemispheric OH is often calculated relative to the hemispheres divided at the equator. This difference is significant and must be considered when comparing estimates of $\langle OH\rangle_n/\langle OH\rangle_s$. For example, in the model described in (*8*), $\langle OH\rangle_n/\langle OH\rangle_s = 1.00$ when the boundary between the hemispheres is set at the equator; this ratio decreases to 0.87 when the Southern Hemisphere is defined as 8°N to 90°S (that is, when one additional model segment, 0° to 8°N, is included as being part of the Southern Hemisphere).
31. J. Rudolph, A. Khedim, R. Koppmann, B. Bonsang, *J. Atmos. Chem.* **22**, 67 (1995).
32. J. Rudolph, personal communication.
33. D. Blake, personal communication.

34. We are indebted to all personnel involved in collecting flask samples at the NOAA/Climate Monitoring and Diagnostics Laboratory (NOAA/CMDL) Observatories and at cooperative sampling sites. S.A.M. acknowledges J. Rudolph for suggesting the approach for determining a Southern Hemispheric lifetime and appreciates insightful discussions with A. Ravishankara, J. Rodriguez, M. Prather, S. Solomon, and S. Yvon-Lewis; the helpful comments of anonymous referees; and the technical assistance of A. Clarke, R. Myers, T. Conway, P. Lang, and N. Paynter. Samples were obtained from PSA with assistance from NOAA's Carbon Cycle group. Supported in part by the Atmospheric Chemistry project of the NOAA Climate and Global Change Program. C.M.S. acknowledges the support of NSF through grants NSF-ATM-9320778 and NSF-ATM-9903529.

7 December 1999; accepted 10 March 2000

Cardiovascular Evidence for an Intermediate or Higher Metabolic Rate in an Ornithischian Dinosaur

Paul E. Fisher,[1*] Dale A. Russell,[2] Michael K. Stoskopf,[3] Reese E. Barrick,[4] Michael Hammer,[5] Andrew A. Kuzmitz[6]

Computerized tomography scans of a ferruginous concretion within the chest region of an ornithischian dinosaur reveal structures that are suggestive of a four-chambered heart and a single systemic aorta. The apparently derived condition of the cardiovascular system in turn suggests the existence of intermediate-to-high metabolic rates among dinosaurs.

The three-chambered heart of modern reptiles (except crocodiles) includes a single ventricle that pumps blood both to the lungs and to the remainder of the body. In crocodiles, the ventricle is composed of two chambers that are incompletely separated from each other functionally by the foramen of Panazzi. Thus, in all living reptiles, oxygenated blood from the lungs and deoxygenated blood from the rest of the body mix together to a greater or lesser extent, reducing the overall oxygen content of blood returned to the body. All modern reptiles have paired systemic aortas arising from the ventricle and distributing blood to the body. In contrast, the four-chambered heart of modern birds and mammals has two completely separated ventricles and a single systemic aorta, ensuring that only completely oxygenated blood is distributed to the body. These modifications to the cardiovascular systems of birds and mammals have been correlated with metabolic rates that are higher than those occurring in living reptiles with their incompletely separated cardiac circulation (*1*).

Much of the discussion about higher metabolic rates in dinosaurs has been focused on saurischian dinosaurs and their role in the origin of birds (*1*–*3*). This has been further stimulated by the recent discovery of hair- or featherlike structures preserved with small theropod (saurischian) skeletons from Cretaceous lake deposits in China (*3*). Ornithischian dinosaurs lack the specializations of some small theropods that suggest high metabolic rates, including enlarged endocranial cavities and complex air-sac systems (*1*). However, by Cretaceous time, complex dental batteries had appeared in two diversified lineages of ornithischians (ornithopods and ceratopsians) (*4*), suggesting a metabolic need to rapidly digest food. Heat flow indicative

[1]Biomedical Imaging Facility, College of Veterinary Medicine, North Carolina State University, 4700 Hillsborough Street, Raleigh, NC 27606, USA. [2]North Carolina State Museum of Natural Sciences and Department of Marine, Earth, and Atmospheric Sciences, North Carolina State University, Raleigh, NC 27695, USA. [3]Department of Clinical Sciences, College of Veterinary Medicine, and Environmental Medicine Consortium, North Carolina State University, Raleigh, NC 27606, USA. [4]Department of Marine, Earth, and Atmospheric Sciences, North Carolina State University, Raleigh, NC 27696, USA. [5]Hammer and Hammer Paleotek, 260 Dutchman View Drive, Jacksonville, OR 97530, USA. [6]595 North Main Street, Ashland, OR 97520, USA.

*To whom correspondence should be addressed. E-mail: Paul_Fisher@ncsu.edu

New Observational Constraints for Atmospheric Hydroxyl on Global and Hemispheric Scales

S. A. Montzka *et al.*

Science **288**, 500 (2000);
DOI: 10.1126/science.288.5465.500

Science (print ISSN 0036-8075; online ISSN 1095-9203) is published weekly, except the last week in December, by the American Association for the Advancement of Science, 1200 New York Avenue NW, Washington, DC 20005.